Characterization of discordance between mismatch repair deficiency and microsatellite instability testing may prevent inappropriate treatment with immunotherapy

Geurts, B.S.; Zeverijn, L.J.; Henegouwen, J.M.V.; Wijngaart, H. van der; Hoes, L.R.; Wit, G.F. de; ... ; Voest, E.E.

Journal of Pathology
J Pathol July 2024; **263:** 288–299
Published online 15 May 2024 in Wiley Online Library
(wileyonlinelibrary.com) DOI: 10.1002/path.6279

ORIGINAL ARTICLE

Characterization of discordance between mismatch repair deficiency and microsatellite instability testing may prevent inappropriate treatment with immunotherapy

Birgit S Geurts[1,2], Laurien J Zeverijn[1,2], Jade M van Berge Henegouwen[3], Hanneke van der Wijngaart[4], Louisa R Hoes[1,2], Gijs F de Wit[1,2], Ilse AC Spiekman[5], Thomas W Battaglia[1,2], Daphne M van Beek[6], Paul Roepman[6], Anne ML Jansen[7], Wendy WJ de Leng[7], Annegien Broeks[8], Mariette Labots[9], Carla ML van Herpen[10], Hans Gelderblom[11], Henk MW Verheul[5], Petur Snaebjornsson[12,13†] and Emile E Voest[1,2*†]

[1] *Division of Molecular Oncology & Immunology, Netherlands Cancer Institute, Amsterdam, The Netherlands*
[2] *Oncode Institute, Utrecht, The Netherlands*
[3] *Department of Clinical Genetics, Erasmus Medical Center, Leiden, The Netherlands*
[4] *Department of Medical Oncology, GROW, Maastricht University Medical Center, Maastricht, The Netherlands*
[5] *Department of Medical Oncology, Erasmus Medical Center, Rotterdam, The Netherlands*
[6] *Hartwig Medical Foundation, Amsterdam, The Netherlands*
[7] *Department of Pathology, University Medical Center Utrecht, Utrecht, The Netherlands*
[8] *Core Facility Molecular Pathology & Biobanking, Netherlands Cancer Institute, Amsterdam, The Netherlands*
[9] *Department of Medical Oncology, Amsterdam UMC, Vrije Universiteit Amsterdam, Cancer Center Amsterdam, Amsterdam, The Netherlands*
[10] *Department of Medical Oncology, Radboud Medical Center, Nijmegen, The Netherlands*
[11] *Department of Medical Oncology, Leiden University Medical Center, Leiden, The Netherlands*
[12] *Department of Pathology, Netherlands Cancer Institute, Amsterdam, The Netherlands*
[13] *Faculty of Medicine, University of Iceland, Reykjavik, Iceland*

**Correspondence to: EE Voest, Division of Molecular Oncology & Immunology, Netherlands Cancer Institute, Plesmanlaan 121, 1066 CX Amsterdam, The Netherlands. E-mail: e.voest@nki.nl*

†These authors shared last author.

Abstract

In the Drug Rediscovery Protocol (DRUP), patients with cancer are treated based on their tumor molecular profile with approved targeted and immunotherapies outside the labeled indication. Importantly, patients undergo a tumor biopsy for whole-genome sequencing (WGS) which allows for a WGS-based evaluation of routine diagnostics. Notably, we observed that not all biopsies of patients with dMMR/MSI-positive tumors as determined by routine diagnostics were classified as microsatellite-unstable by subsequent WGS. Therefore, we aimed to evaluate the discordance rate between routine dMMR/MSI diagnostics and WGS and to further characterize discordant cases. We assessed patients enrolled in DRUP with dMMR/MSI-positive tumors identified by routine diagnostics, who were treated with immune checkpoint blockade (ICB) and for whom WGS data were available. Patient and tumor characteristics, study treatment outcomes, and material from routine care were retrieved from the patient medical records and via Palga (the Dutch Pathology Registry), and were compared with WGS results. Initially, discordance between routine dMMR/MSI diagnostics and WGS was observed in 13 patients (13/121; 11%). The majority of these patients did not benefit from ICB (11/13; 85%). After further characterization, we found that in six patients (5%) discordance was caused by dMMR tumors that did not harbor an MSI molecular phenotype by WGS. In six patients (5%), discordance was false due to the presence of multiple primary tumors ($n = 3$, 2%) and misdiagnosis of dMMR status by immunohistochemistry ($n = 3$, 2%). In one patient (1%), the exact underlying cause of discordance could not be identified. Thus, in this group of patients limited to those initially diagnosed with dMMR/MSI tumors by current routine diagnostics, the true assay-based discordance rate between routine dMMR/MSI-positive diagnostics and WGS was 5%. To prevent inappropriate ICB treatment, clinicians and pathologists should be aware of the risk of multiple primary tumors and the limitations of different tests.

Keywords: microsatellite instability; immune checkpoint blockade; mismatch repair deficiency; immunohistochemistry; polymerase chain reaction; whole-genome sequencing

Received 9 October 2023; Revised 18 January 2024; Accepted 29 February 2024

Conflict of interest statement: EEV has, through the Drug Rediscovery Protocol (DRUP), received support from pharmaceutical companies participating in DRUP, including Bristol Myers Squibb and AstraZeneca. PS has carried out unrelated consultancy for Merck Sharp & Dohme and Bayer, and has received payments from MEDtalks for educational presentations. No other conflicts of interest were declared.

Introduction

The mismatch repair (MMR) system is a DNA repair mechanism that ensures genomic stability by detecting and repairing single-base mismatches and insertions and deletions (indels) that occur during DNA replication and recombination. Mismatch repair deficiency is caused by germline or somatic alterations in one of the four major MMR genes (*MLH1*, *MSH2*, *MSH6*, and *PMS2*) or epigenetic alterations, most commonly being an *MLH1* promoter hypermethylation [1,2]. This will lead to the accumulation of single-base substitutions (SBS) and indels in highly repetitive DNA sequences, termed microsatellites, resulting in high tumor mutational burden (TMB) and variable microsatellite length, which is termed microsatellite instability (MSI) [3,4]. MSI occurs in approximately 2–4% of all diagnosed cancers [1] and is most often observed in colorectal cancer (CRC) and endometrial cancer (EC) but can also be found in many other tumor types [1,5].

In daily clinical practice, MMR and MSI testing are performed by immunohistochemistry (IHC) or DNA-based molecular analysis, respectively. IHC evaluates the immunohistochemical staining of the four major MMR proteins. A tumor is considered to be mismatch repair-deficient (dMMR) if loss of nuclear expression of at least one MMR protein is observed [5]. DNA-based molecular analysis is mainly based on the polymerase chain reaction (PCR), detecting the level of instability in a panel of five microsatellites [6–8]. Generally, a tumor is classified as microsatellite-unstable by PCR if at least two out of five routinely tested microsatellites are unstable [5]. IHC is the preferred primary screening test, due to its lower costs, faster turnaround time, and broad availability in routine diagnostic laboratories. Other DNA-based molecular tests, such as next-generation sequencing (NGS) and whole-genome sequencing (WGS), are also increasingly used as part of a broad diagnostic workup. These tests identify substantially more microsatellites compared with PCR and can determine both MSI status and various genomic alterations simultaneously. Both MMR and MSI testing are considered to be very sensitive with high concordance: from 95% to nearly 99% for CRC [6,9–12] and from 91% to 95% in non-CRC [13–16].

MMR/MSI testing was traditionally performed in patients with CRC or EC to screen for Lynch syndrome (LS) [17], as ∼20% of the dMMR/MSI tumors arise in patients with LS [18]. However, dMMR/MSI has been established as a strong biomarker to predict the efficacy of immune checkpoint blockade (ICB) [3,19,20]. Various regulatory approvals have now been granted for ICB treatment in patients with a variety of dMMR/MSI tumors [21,22]. Consequently, MMR/MSI testing is increasingly integrated into the routine care of patients with various types of solid tumors. Given the clinical importance and the observation that dMMR/MSI misdiagnosis is an important primary ICB resistance mechanism [23], accurate determination of MMR/MSI status is crucial in identifying patients most likely to benefit from ICB and to avoid inappropriate treatment with expensive and potentially harmful ICB drugs.

Within the Drug Rediscovery Protocol (DRUP), patients with advanced solid tumors without standard-of-care treatment options are treated based on their tumor molecular profile with approved therapies outside the registered indication. Importantly, patients undergo a mandatory pre-treatment tumor biopsy for WGS, which allows for a WGS-based evaluation of routine diagnostics. Remarkably, in a subset of patients who were included based on dMMR/MSI as determined by routine diagnostics and treated with ICB, subsequent WGS did not classify their biopsies as microsatellite-unstable. Therefore, we aimed to evaluate the discordance rate between routine dMMR/MSI diagnostics and WGS and to further characterize discordant cases.

Materials and methods

Ethics approval and patient consent statement

DRUP was approved by the independent Medical Ethical Committee of the Netherlands Cancer Institute in Amsterdam and by the Institutional Review Boards in every participating hospital. The study was conducted in accordance with Good Clinical Practice guidelines and the Declaration of Helsinki's ethical principles for medical research. Written informed consent was obtained from all study subjects. This substudy was performed with the approval of the Institutional Review Board of the Netherlands Cancer Institute in Amsterdam (IRBdm21-252).

Study design and study population

Adult patients with advanced dMMR/MSI solid tumors identified by IHC and/or DNA-based molecular tests (PCR/NGS) during routine care, and from whom WGS data were available from the mandatory pre-treatment biopsy in DRUP, were selected and retrospectively analyzed. Upon inclusion in DRUP, patients received ICB monotherapy, including nivolumab or durvalumab. Clinical benefit was defined by confirmed complete or partial response or stable disease ≥16 weeks, according to Response Evaluation Criteria in Solid Tumors Version 1.1 [24].

Patient and tumor characteristics

Patient and tumor characteristics, and study treatment outcomes were collected as part of the DRUP electronic case report form. Pathology reports and corresponding formalin-fixed, paraffin-embedded (FFPE) tissue, slides, and stains from routine care were retrieved via the nationwide network and registry of histo- and cytopathology in The Netherlands (Palga) [25].

Whole-genome sequencing

WGS was performed by the Hartwig Medical Foundation (Amsterdam, The Netherlands; hereafter referred to as Hartwig). DNA was isolated from tumor biopsies and from matching blood samples. If the molecular-based tumor cell percentage was ≥20% and the DNA yield was ≥300 ng, WGS was performed on the Illumina NovaSeq 6000 (Illumina, San Diego, CA, USA) platform (2 × 151 bp reads) with median sequencing depths of ∼100× and 40× for tumor and blood, respectively. In brief, reads were aligned to the reference genome GRCh37 and further processed using Hartwig's in-house tools [26,27], whereby somatic single nucleotide variants and indels were called using SAGE. TMB per megabase (Mb), tumor mutational load (TML), and MSI scores were calculated by computing the number of total somatic mutations, the number of missense mutations, and the number of indels per million bases occurring in homopolymers of five or more bases or di-, tri-, and tetra-nucleotide sequences of repeat count four or more, respectively. Samples with an MSI score of ≥4 were considered to be microsatellite-unstable (MSI-positive). SBS mutational signatures associated with dMMR/MSI were determined using the mutationalPatterns package [26,28,29].

Discordant cases

All cases with discordance between routine dMMR/MSI diagnostics and WGS-based MSI status were individually evaluated by an experienced pathologist and medical doctor. If available, original stains from routine care [hematoxylin and eosin (H&E) stains, immunohistochemical stains] were re-evaluated. After comprehensively reviewing each case, a hypothesis explaining the discordance was formulated. Based on this hypothesis, it was decided if and which additional tests were necessary to confirm or reject the hypothesis. WGS data were extensively evaluated in all cases. If the presence of multiple primary tumors (MPTs) was hypothesized, the cancer of unknown primary prediction algorithm (CUPPA) was performed as previously described [30].

Immunohistochemistry

If FFPE material was available and misdiagnosis of routine diagnostics was hypothesized, MMR IHC was (re) performed on a Ventana BenchMark ULTRA autostainer (Roche Diagnostics, Almere, The Netherlands). In brief, paraffin sections were cut at 3 µm, heated at 75 °C for 28 min, and deparaffinized in the instrument with EZ prep solution (Roche Diagnostics). Heat-induced antigen retrieval was carried out using Cell Conditioning 1 (CC1, Roche Diagnostics) for 32 min at 95 °C (MSH2 and MSH6) or 64 min at 95 °C (MLH1 and PMS2). MLH1, MSH2, MSH6, and PMS2 were detected using clone M1 (Ready-to-Use, 8 min at 37 °C, Cat. No. 8033668001, Roche Diagnostics), clone G219-1129 (Ready-to-Use, 12 min at 37 °C, Cat. No. 8033684001, Roche Diagnostics), clone EP49 (1/25 dilution, 32 min at 37 °C, Cat. No. AC0047EU; Epitomics, Burlingame, CA, USA), and clone EP51 (1/10 dilution, 32 min at 37 °C, Cat. No. M3647; Agilent Technologies Netherlands, Amstelveen, The Netherlands), respectively. Bound antibody was visualized using the OptiView DAB Detection Kit (Roche Diagnostics). Slides were counterstained with Hematoxylin and Bluing Reagent (Roche Diagnostics). To scan the slides at a 40× objective magnification, a PANNORAMIC® 1000 scanner from 3DHISTECH (Budapest, Hungary) was used.

Tumors with absent nuclear staining of one or more MMR proteins were considered to be dMMR when adequate internal and external controls were present. If no loss of expression of MMR proteins was observed, tumors were classified as mismatch repair-proficient (pMMR).

DNA-based molecular analysis

In one case, additional DNA-based molecular analysis was carried out to confirm the hypothesis of misdiagnosis. The pathologist scored the tumor percentage and indicated the most tumor-dense region for isolation on an H&E stain using Slidescore (https://www.slidescore.com). DNA was isolated from 10-µm FFPE slides using the AllPrep DNA/RNA FFPE isolation kit (Cat. No. 80234; QIAGEN Venlo, The Netherlands) by using the QIAcube (QIAGEN), according to the manufacturer's protocol. Mutation status was evaluated using a Custom Illumina AmpliSeq panel (Illumina) using the standardized protocol as used in diagnostic settings. The following genes were sequenced: *EPCAM* (exons 8 and 9, intron 8), *MLH1* (exons 1–19), *MSH2* (exons 1–16), *MSH6* (exons 1–10), and *PMS2* (exons 1–11). Also, MSI analysis was included in the same sequencing panel using 65 microsatellite loci. Microsatellite (in) stability was determined by mSINGS (Illumina, PMID 24987110). MSI-positivity was defined as instability at ≥30% of evaluated loci.

Statistical analysis

All statistical analyses were performed using SPSS version 29.0 (SPSS Inc., Chicago, IL, USA) and R version 4.0.3 (The R Foundation for Statistical Computing, Vienna, Austria).

Results

General characteristics

From September 2016 through April 2022, 209 patients with a dMMR/MSI tumor were included in DRUP and treated with ICB. After excluding patients who were referred based on WGS evaluation or LS, and thus had no other routine diagnostics available ($n = 10$) or for whom no WGS data were available due to any reasons ($n = 78$), 121 patients were included in this study (Figure 1). The majority of patients were diagnosed with colorectal ($n = 57$, 47%), endometrial ($n = 16$, 13%), or

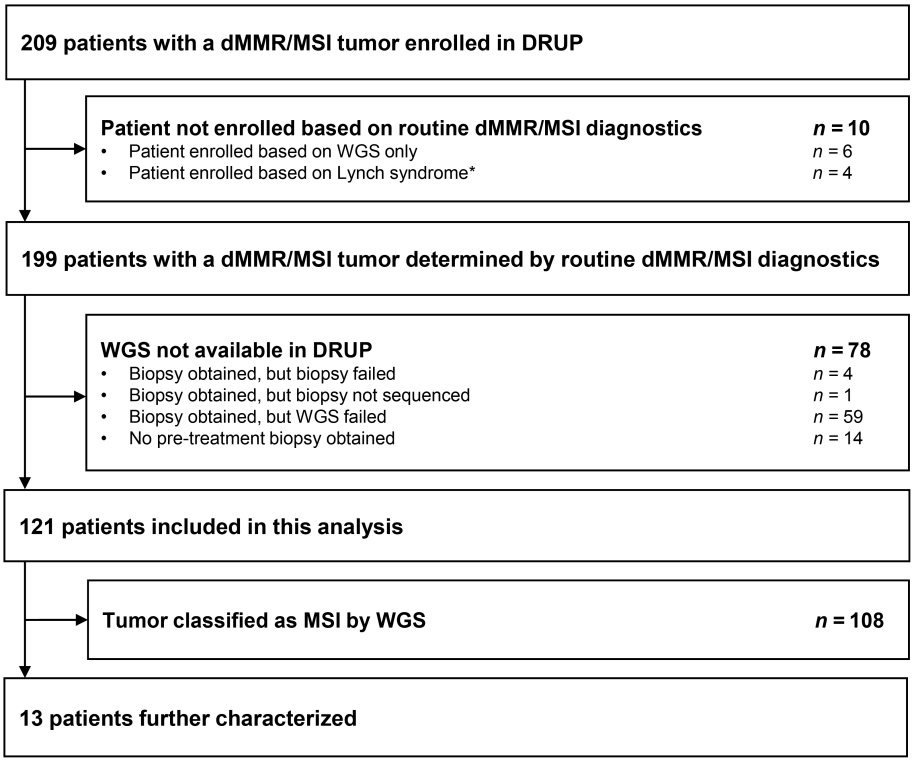

Figure 1. Flowchart of the enrollment of patients in this study, displaying reasons for excluded patients. *In patients enrolled based on Lynch syndrome, WGS in DRUP showed MSI. dMMR, mismatch repair-deficient; DRUP, Drug Rediscovery Protocol; MSI, microsatellite instability; WGS, whole-genome sequencing.

prostate cancer ($n = 12$, 10%). Patients' and tumor characteristics are summarized in Table 1.

Test results of routine dMMR/MSI diagnostics prior to DRUP inclusion are shown in Table 2. MMR testing was performed in 117 patients (117/121, 97%) and the majority of patients showed combined loss of MLH1/PMS2 expression ($n = 72$, 72/121, 60%). MSI testing was performed in a subset of patients ($n = 44$, 44/121, 36%). In 40 patients (40/121, 33%), both MMR and MSI testing were performed.

Routine analyses were mainly performed on primary tumors, while WGS on pre-treatment biopsies in DRUP was mainly performed on metastases (Table 2). In 108 patients (108/121, 89%), WGS demonstrated MSI (Table 2). The median MSI score, TMB, and TML of these patients were 93 (range 6–343), 143 (range 15–457) mut/Mb, and 1,116 (range 206–10,040) missense mutations per genome, respectively. The average contribution of dMMR/MSI-associated mutational signatures in WGS-based MSI tumors is presented in supplementary material, Table S1.

In 13 patients (13/121, 11%), the previously established dMMR/MSI status was not confirmed by WGS (Table 3). In seven of these, discordance between different tests was already observed during routine care (7/13, 54%, Table 3). The majority of these patients (11/13, 85%, Table 3) did not benefit from ICB. All discordant cases are further described below and classified according to different categories.

Mismatch repair deficiency does not always lead to the presence of an MSI molecular phenotype

In six patients (46% of discordant cases and 5% of all patients), discordance was caused by dMMR tumors that did not harbor an MSI molecular phenotype (cases 1–6, Table 3). Notably, two patients (2/6, 33%) achieved durable clinical benefit from nivolumab.

Three patients in this category had LS. They had pancreatic cancer (case 1, Table 3), peritoneal mesothelioma (case 2, Table 3), and cancer of unknown primary (case 3, Table 3). Routine analysis showed isolated loss of MSH6 expression (cases 1 and 2, Table 3) and combined loss of MSH2/MSH6 expression (case 3, Table 3). WGS indicated microsatellite stability (MSS), but the MSI score was close to the cut-off point of 4 in two patients (MSI score of 3.39 and 2.07 in cases 1 and 3, respectively). However, TML and the contribution of SBS6 (cases 1 and 2, supplementary material, Table S2) and SBS15 (case 3, supplementary material, Table S2) were relatively high. These findings indicate that these tumors were dMMR secondary to LS, but did not harbor a clear MSI molecular phenotype.

Two patients in this category had metastatic EC. In the first patient (case 4, Table 3), the primary tumor showed tumor heterogeneity with some areas demonstrating clonal loss of MLH1/PMS2 expression with MSI secondary to *MLH1* promoter hypermethylation, while other areas showed retained expression of MMR proteins with MSS. We confirmed this by repeating IHC

Table 1. General characteristics of included patients.

Characteristics	Number (%) out of 121 patients	
Median age at diagnosis (IQR), years	66	(57–73)
Gender, *n* (%)		
Male	62	51%
Female	59	49%
Primary tumor location, *n* (%)		
Colorectum	57	47%
Endometrium	16	13%
Prostate	12	10%
Biliary tract	8	7%
Stomach	8	7%
Small intestine	7	6%
Breast	2	2%
Unknown primary	2	2%
Esophagus	2	2%
Pancreas	2	2%
Brain	1	1%
Bladder	1	1%
Cervix	1	1%
Mesothelioma	1	1%
Sarcoma	1	1%
Metastases, *n* (%)		
Yes, metachronous (>6 months after primary diagnosis)	57	47%
Yes, synchronous	55	45%
No	9	7%
Lynch syndrome, *n* (%)	25	21%
Treatment in DRUP, *n* (%)		
Nivolumab	105	87%
Durvalumab	16	13%
Best overall response to immune checkpoint blockade		
Complete response	7	6%
Partial response	42	35%
Stable disease	23	19%
Progressive disease	36	30%
Not evaluable	13	11%

Percentages may not equal 100% due to rounding.

Table 2. Results of routine dMMR/MSI diagnostics and WGS of included patients.

Total, *n*	121	
dMMR/MSI routine diagnostics, *n* (%)		
IHC only	77	64%
IHC and PCR	34	28%
IHC and NGS	4	3%
PCR only	2	2%
IHC, PCR, and NGS	2	2%
PCR and NGS	1	1%
NGS only	1	1%
IHC during routine diagnostics, *n* (%)		
Total	117	97%
Loss of MLH1/PMS2 expression	72	60%
Loss of MSH2/MSH6 expression	18	15%
Isolated loss of MSH6 expression	10	8%
Isolated loss of PMS2 expression	8	7%
Other loss of MMR protein expression*	7	6%
Discordance†	2	2%
PCR during routine diagnostics, *n* (%)		
Total	38	31%
MSI	31	26%
MSS‡	6	5%
Discordance§	1	1%
NGS during routine diagnostics, *n* (%)		
Total	8	7%
MSI	7	6%
Dubious	1	1%
Routine diagnostics performed on ..., *n* (%)		
Primary tumor	66	55%
Metastasis	29	24%
Both	26	21%
Methylation of *MLH1* gene promoter, *n* (%)		
Presence	48	40%
Absence	18	15%
Not tested	53	44%
Not evaluable	2	2%
WGS in DRUP performed on ..., *n* (%)		
Metastasis	101	83%
Primary tumor	19	16%
Missing data	1	1%
WGS-based MSI status in DRUP, *n* (%)		
MSI	108	89%
MSS	13	11%

IHC, immunohistochemistry; MSI, microsatellite instability; MSS, microsatellite stability; NGS, next-generation sequencing; PCR, polymerase chain reaction; WGS, whole-genome sequencing.
*Isolated loss of MSH2 expression ($n = 2$), loss of MSH6/PMS2 expression ($n = 2$), loss of MLH1/PMS2/MSH2 expression ($n = 1$), loss of MLH1/PMS2/MSH6 expression ($n = 1$), and isolated loss of MLH1 expression ($n = 1$).
†In one case, the primary tumor (gastric carcinoma) showed loss of MLH1/PMS2 expression and a liver metastasis showed retained expression of MMR proteins. In one case, there were two primary tumors (colorectal carcinomas) of which one tumor showed loss of MLH1/PMS2 expression and one tumor showed retained expression of MMR proteins.
‡In four cases, PCR and WGS were concordant, both showing MSS. In two cases, PCR showed MSS, while WGS showed MSI. These two cases are not described in detail.
§PCR showed MSI in regions with loss of MLH1/PMS2 expression and MSS in regions with retained expression of MMR proteins.

(Figure 2A,B). WGS, performed on a liver metastasis, indicated MSS, but the MSI score was close to the cut-off point of 4 (MSI score of 3.62). Additionally, the contribution of SBS26 and SBS44 was relatively high (supplementary material, Table S2). We subsequently performed IHC on the same metastasis and observed heterogeneous loss of MLH1 expression and complete loss of PMS2 expression (Figure 2C).

In the second patient with EC (case 5, Table 3), the primary tumor showed loss of MLH1/PMS2 expression without *MLH1* promotor hypermethylation and MSS. Routine analysis of a metastatic lesion in the abdominal wall showed loss of MLH1/PMS2 expression, which we confirmed upon re-evaluation. WGS, performed on a different metastasis in the abdominal wall, also showed MSS. We subsequently performed IHC on that metastasis and observed loss of MLH1/PMS2 expression. Interestingly, we could not identify an underlying cause of the dMMR status.

The last patient in this category had metastatic esophageal squamous cell carcinoma (case 6, Table 3). The primary tumor showed loss of MLH1/PMS2 expression without *MLH1* promotor hypermethylation and MSS. We repeated IHC and found heterogeneous loss of expression of MLH1/PMS2. WGS, performed on a liver metastasis, also showed MSS, while the contribution of SBS6 was relatively high (supplementary material, Table S2). We subsequently performed IHC on the same liver metastasis, which was suspicious for isolated loss of PMS2 expression. Similar to case 5, we could not identify an underlying cause of the dMMR status.

Table 3. Characteristics of discordant cases.

Clinical characteristics						
Case	**Sex**	**Age at diagnosis (years)**	**Origin**	**Histology**	**Lynch mutation**	**BOR to ICB**
1	M	78	Pancreas	Adenocarcinoma	*MSH6* p.Ser156*	PD
2	M	44	Peritoneum	Mesothelioma	*MSH6* p.Arg1005*	PR
3	M	69	Unknown primary	Undifferentiated malignant neoplasm	*MSH2* p.Glu878fs	PR
4	F	55	Endometrium	Adenocarcinoma		PD
5	F	60	Endometrium	Adenocarcinoma		PD
6	M	82	Esophagus	Squamous cell carcinoma		PD
7	M	75	Colorectum	Adenocarcinoma		PD
8	F	73	Colorectum	Adenocarcinoma		PD
9	F	70	Colorectum	Adenocarcinoma		PD
10	F	77	Colorectum	Adenocarcinoma		PD
11	F	76	Endometrium	Carcinosarcoma		PD
12	M	44	Ampulla of Vater	Adenocarcinoma		PD
13	M	73	Stomach	Adenocarcinoma		PD

Case	**Routine IHC testing**			**Routine PCR testing**[†]		***MLH1* promoter hypermethylation**
	Tissue	**Result**	**Pattern**	**Tissue**	**Result**	
1	Metastasis – lung	dMMR	Isolated MSH6 loss	NA	NA	NA
2	Metastasis – peritoneum	dMMR	Isolated MSH6 loss	Metastasis – peritoneum	MSS	NA
3	Metastasis – abdominal mass	dMMR	MSH2/MSH6 loss	NA	NA	NA
4	Primary	dMMR	MLH1/PMS2 loss	Primary	MSI	Present
				Primary	MSS	
5	Primary	dMMR	MLH1/PMS2 loss	Primary	MSS	Absent
	Metastasis – abdominal wall	dMMR	MLH1/PMS2 loss	Primary	MSS	
6	Primary	dMMR	MLH1/PMS2 loss	Primary	MSS	Absent
7	Primary (tumor 1)	dMMR	MLH1/PMS2 2 loss	Primary (tumor 1)	MSI	Present
	Primary (tumor 2)	pMMR	No loss	NA	NA	
	Metastasis – adrenal gland	dMMR	MLH1/PMS2 loss	NA	NA	
8	Primary	dMMR	MLH1/PMS2 loss	Primary	MSI	Present
9	Primary	dMMR	MLH1/PMS2 loss	NA	NA	NA
10	Primary	dMMR	Isolated MSH6 loss	NA	NA	NA
11	Primary	dMMR	Isolated MLH1 loss	NA	NA	NA
12	Primary	dMMR	MLH1/PMS2 loss	NA	NA	Absent
13	Primary	dMMR	MLH1/PMS2 loss	NA	NA	NA
	Metastasis – liver	pMMR	No loss	Metastasis – liver	MSS	

Whole-genome sequencing							
Case	**Tissue**	**MSI score**	**TMB (mut/Mb)**	**TML**	**MMR somatic variant**	**Class**[‡]	**Reason for discordance**
1	Metastasis – lung	3.39	21.84	727			dMMR without an MSI molecular phenotype
2	Metastasis – peritoneum	0.86	10.14	373			dMMR without an MSI molecular phenotype
3	Metastasis – mass upper abdomen	2.07	7.27	189	*MLH1* p.Arg385His; *MSH6* p.Arg1005*	3	dMMR without an MSI molecular phenotype
4	Metastasis – liver	3.62	7.28	78	*MSH6* p.Pro1086fs	5	dMMR without an MSI molecular phenotype
5	Metastasis – abdominal wall	0.28	3.6	73			dMMR without an MSI molecular phenotype
6	Metastasis – liver	0.20	4.87	95	*PMS2* p.Lys651Glu	3	dMMR without an MSI molecular phenotype
7	Metastasis – liver	0.38	12.26	127			Multiple primary tumors
8	Metastasis – peritoneum	0.44	4.83	77			Multiple primary tumors
9	Metastasis – vulva	0.09	2.03	38			Multiple primary tumors
10	Metastasis – liver	0.65	9.19	172			Misdiagnosis
11	Metastasis – peritoneum	0.10	3.71	71			Misdiagnosis
12	Metastasis – liver	0.32	8.63	172	*MLH1* p.Arg575Gly[§]	3	Misdiagnosis
13	Metastasis – liver	0.05	2.12	33	*MSH6* p.Lys1352Thr	3	Unsolved

BOR, best overall response; dMMR, mismatch repair-deficient; F, female; ICB, immune checkpoint blockade; IHC, immunohistochemistry; M, male; MMR, mismatch repair; MSI, microsatellite instability; MSS, microsatellite stability; mut/Mb, mutations per megabase; NA, not applicable; PCR; polymerase chain reaction; PD, progressive disease; pMMR, mismatch repair-proficient; PR, partial response; TMB, tumor mutational burden; TML, tumor mutational load.

[†]In all cases in which PCR was performed, pentaplex was used.

[‡]Prediction of pathogenicity in MMR somatic variant [benign (1), likely benign (2), uncertain (3), likely pathogenic (4), definitely pathogenic (5)].

[§]Bi-allelic in tumor.

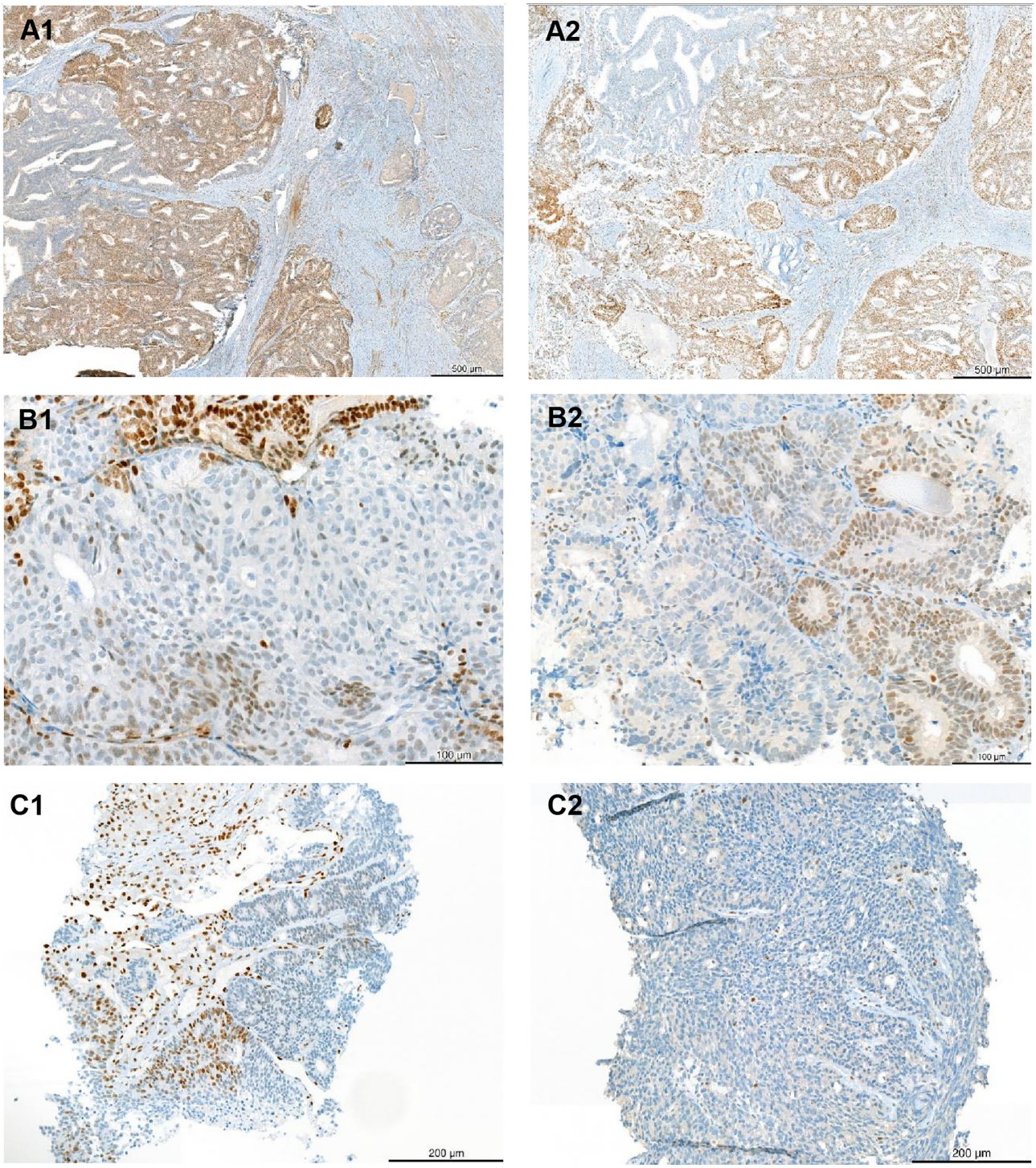

Figure 2. Heterogeneous loss of MLH1/PMS2 expression in case 4. (A1) MLH1 and (A2) PMS2 staining on resection material of the primary tumor (endometrial carcinoma) showed subclonal loss of expression of MLH1 and PMS2. (B1) MLH1 and (B2) PMS2 staining on a biopsy of the primary tumor (endometrial carcinoma) showed heterogeneous loss of expression of MLH1 and PMS2. (C1) MLH1 and (C2) PMS2 staining on a biopsy of a liver metastasis showed heterogeneous loss of expression of MLH1 and complete loss of expression of PMS2.

Different driver mutations in primary tumors and metastases indicate the presence of multiple primary tumors

In three patients with CRC (23% of discordant cases and 2% of all patients), discordance was false and caused by the presence of MPTs (cases 7–9, Table 3). None of these patients experienced clinical benefit from ICB.

The first patient in this category (case 7, Table 3) had two primary CRCs, one of which had metastasized. One tumor was dMMR, while the other was pMMR, which we confirmed by repeating IHC. We identified a clonal relationship between the liver metastasis used for WGS and the primary pMMR tumor based on the same exact combination of mutations in *KRAS* and *PIK3CA*.

In the remaining two patients in this category (cases 8 and 9, Table 3), the primary tumors showed loss of MLH1/PMS2 expression and a *BRAF* V600E mutation. In one of these patients (case 8), we could not re-evaluate the MMR status as tissue and original immunohistochemical stains were not available. However, IHC had been reassessed during routine care, making misdiagnosis unlikely. In the other patient (case 9), we confirmed loss of MLH1/PMS2 expression by repeating IHC. In both patients, WGS was performed on a biopsy of a liver metastasis and revealed no *BRAF* V600E mutation, but instead different driver mutations. As *BRAF* V600E mutations usually occur early in CRC carcinogenesis [31] and the molecular profile was different with regard to both MMR status and driver mutation profile, we considered a clonal relationship between the primary tumor and metastasis unlikely. In addition, the WGS-CUPPA algorithm did not predict CRC, but an upper gastrointestinal tumor in both patients.

Misdiagnosis of MMR status by IHC caused by poor fixation or inadequate staining procedure

In three patients (23% of discordant cases and 2% of all patients), discordance was false and caused by misdiagnosis of dMMR status by IHC (cases 10–12, Table 3). None of these patients experienced clinical benefit from ICB.

The first patient in this category had CRC (case 10, Table 3). IHC was originally interpreted as isolated loss of MSH6 expression, but we found upon re-evaluation morphological and immunohistochemical signs of poor fixation (Figure 3A). Subsequently, we repeated IHC on the same tissue block from the primary tumor and a peritoneal metastasis and found intact expression of MMR proteins nearest to the surface, with gradation of diminishing expression towards the center (Figure 3B,C). The findings were consistent with both suboptimal fixation and low antibody concentration, leading to erroneous interpretation of the MMR status.

The second patient in this category had EC (case 11, Table 3). IHC was originally interpreted as isolated loss of MLH1 expression, but we found complete lack of staining throughout the whole tissue, i.e. both in tumor cells and in the internal control during re-evaluation, indicating a failed staining procedure (no reactivity in non-neoplastic cells). The corresponding tissue block of the primary tumor could not be retrieved for repeating IHC, and we therefore performed IHC on a peritoneal metastasis, revealing intact expression of MMR proteins in both tumor and normal tissue.

The third and last patient in this category had ampullary carcinoma (case 12, Table 3). As the original immunohistochemical stains were not available, we repeated IHC on the primary tumor. Both morphology and the immunohistochemical staining patterns were indicative of poor fixation of the resection specimen, with all MMR stains showing suboptimal staining and gradation of staining intensity (MLH1, MSH2, and MSH6: some positivity present; PMS2 inconclusive), with loss of staining mainly centrally in both tumor cells and the internal control. Due to the poor staining quality, we additionally performed DNA-based molecular analysis on the primary tumor, which showed MSS without any alterations in MMR genes. Furthermore, we performed IHC on a liver metastasis, which showed intact expression of all four MMR proteins, all indicative of a valid MSS classification by WGS.

Unsolved case

In one patient (8% of discordant cases and 1% of all patients), we could not identify the exact underlying cause for discordance between routine diagnostics and WGS. Hence, it remains uncertain if discordance was true or false.

This patient (case 13, Table 3) had metastatic gastric carcinoma. Routine analysis on the primary tumor showed loss of MLH1/PMS2 expression, while a liver metastasis was classified as pMMR, which we confirmed upon re-evaluation. WGS, performed on the same liver metastasis, showed MSS and several mutations, including a *BAP1* mutation. Unfortunately, the tissue block from the primary tumor on which the MMR staining was performed was not available for clonality analysis. However, *BAP1* mutations are relatively rare in gastric cancers and occur more frequently in intrahepatic cholangiocarcinoma [32]. The WGS-CUPPA algorithm, however, was inconclusive. Thus, this case may represent false discordance due to the presence of MPTs but could also represent tumor heterogeneity of MMR/MSI status between the primary tumor and liver metastasis.

In conclusion, in these patients initially diagnosed with dMMR/MSI tumors by routine diagnostics, the true assay-based discordance rate between routine dMMR/MSI diagnostics and WGS after re-evaluating was 5% (6/121).

Discussion

In the paradigm of precision oncology, accurate determination of molecular profiles, such as dMMR/MSI, is essential. While IHC and PCR are currently routinely used for MMR and MSI testing, respectively, WGS has emerged as a promising alternative, showing a sensitivity of 100% and a specificity of 94% across different tumor types [27] and determining both MSI status and various other genomic alterations that result from MMR inactivation (such as increased TMB/TML). Hence, we considered WGS as the ultimate test to evaluate current routine dMMR/MSI diagnostics.

In our study, we found a relatively low true assay-based discordance rate of 5% between routine dMMR/MSI diagnostics and WGS, which aligns with previous literature reporting discordance rates between different MMR/MSI tests across solid tumors [6,9–15]. True discordance was caused by dMMR tumors that did not harbor an MSI molecular phenotype (cases 1–6). This profile has been previously described in various tumor types and occurs most commonly in non-

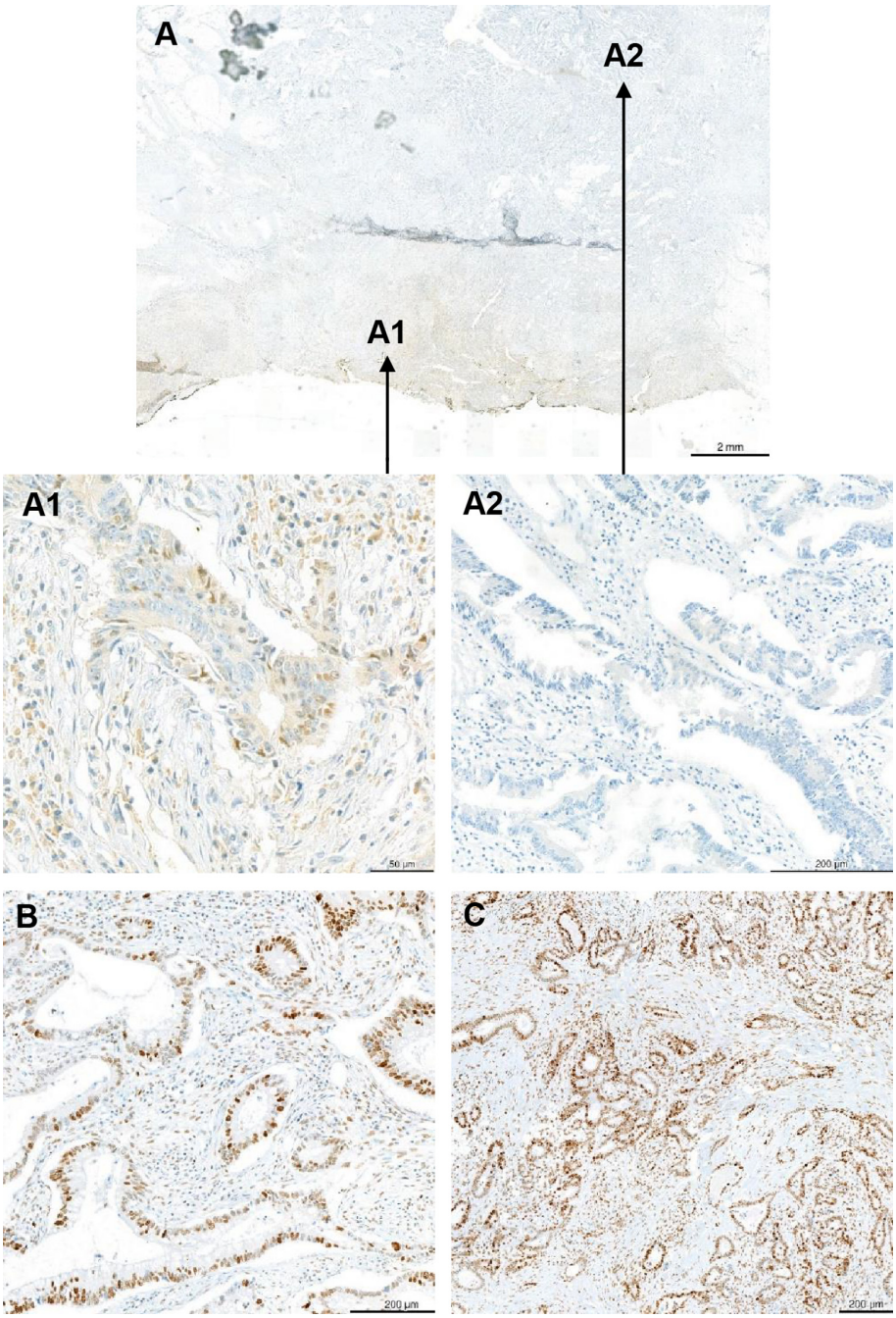

Figure 3. Suboptimal fixation and low antibody concentration leading to erroneous interpretation of MMR status in case 10. Panel A shows an original MSH6 staining carried out on the primary tumor (colorectal carcinoma) during routine diagnostics. There are signs of poor fixation, i.e. hardly any staining of normal internal control (A1, A2) and retraction artefacts around tumor glands and fragmentation of epithelium (A2). Towards the periphery of the slide (closest to the earliest fixation), there was minimal MSH6 expression appreciable in a few tumor cells (A1), while centrally there was complete lack of staining, both in tumor cells and in the internal control (A2). IHC repeated on the same tissue block from the primary tumor (colorectal carcinoma) using our own routine staining protocol (see the Materials and methods section) demonstrated increased but heterogeneous loss of MSH6 expression in the periphery of the slide, both in tumor cells and in the internal control (B), indicating that the antibody concentration was too low in the original staining procedure. Additionally, we performed IHC on a peritoneal metastasis from the tumor, which also showed intact MSH6 expression (C).

CRC [33], which is consistent with our findings. Factors that may explain this profile include the role of tissue of origin (including microenvironment) and the functional effect of the exact bi-allelic MMR inactivation, which varies depending on the MMR protein and the type of DNA alteration [5,33–35]. Although previous studies have suggested that these tumors are less sensitive to ICB compared with dMMR/MSI tumors [33,36], our data show that some were sensitive to ICB, likely due to other characteristics that result from MMR inactivation, mainly high TMB/TML. This suggests that ICB treatment outcomes in these patients may be improved by making treatment decisions in conjunction with other biomarkers, rather than only dMMR/MSI status.

Although we considered WGS as the ultimate test to evaluate routine dMMR/MSI diagnostics, this method also has limitations, such as a high error rate for sequencing long microsatellites [37] and the inclusion of di-, tri-, and tetra-nucleotide repeats [38]. These repeats exhibit a lower sensitivity for detecting MSI than mononucleotide repeats, especially in MSH6-deficient tumors [38]. Furthermore, the detection limit varies across MSI testing methods [39], possibly leading to discordance between different tests. Therefore, it is important to collectively consider other biomarkers that result from MMR inactivation, including increased TMB/TML, SBS mutational signatures, and the presence of pathogenic variants in MMR genes, for a correct diagnosis when performing (WGS-based) MSI testing.

Strikingly, in two dMMR tumors without an MSI molecular phenotype (cases 5 and 6), we could not identify an underlying cause for the dMMR status after eliminating common explanations. Therefore, we posit that a deficient MMR system in some cases may be driven by genetic alterations affecting a gene other than MMR genes, or that epigenetic alterations in genes not covered by our analyses may contribute to the pathogenesis of dMMR tumors without an MSI molecular phenotype, necessitating further investigation.

In three tumors (cases 4–6), heterogeneous loss of expression of MMR proteins was observed, indicating tumor heterogeneity. The reasons for tumor heterogeneity are unknown but may reflect subclonal variation in MMR gene inactivation or heterogeneity of *MLH1* promoter hypermethylation [40]. At present, the exact incidence and therapeutic consequences of dMMR/pMMR tumor heterogeneity remain unclear. Hence, additional studies are needed to improve our biological understanding of tumor dMMR/pMMR heterogeneity.

Furthermore, false discordance caused by MPTs occurred in 2% of patients (cases 7–9). This phenomenon is not rare and has been described in 2–17% of patients with cancer [41]. Notably, none of these patients experienced clinical benefit from ICB, underscoring the importance of clinically recognizing them. Clinical features such as atypical metastatic spread, new metastases several years after a primary cancer diagnosis, a medical history of MPTs, and suspicious lesions on radiological imaging should alert clinicians [41]. MMR/MSI testing of multiple lesions should then be considered to make accurate treatment decisions. Additionally, clinicians should be aware of the fact that unexpected outcomes to ICB treatment may reflect the presence of MPTs.

In another 2% of patients (cases 10–12), false discordance was caused by misdiagnosis of dMMR status by IHC. Thus, the diagnostic error rate seems to be low. Nevertheless, given the significant impact of misdiagnosis at the individual level, efforts could be made to further improve IHC quality. These include optimization of tissue acquisition and processing to avoid poor fixation as well as providing good training to pathologists to ensure adequate interpretation. To this end, it is important that pathologists are aware of the morphological signs of poor fixation as well as suboptimal staining (too low antibody concentration) or failed staining procedure (complete lack of staining). In the presence of weak expression or unusual staining patterns, additional tests and re-assessment are required.

The current ESMO guideline recommends both IHC and PCR in LS-related cancers when ICB eligibility is assessed [42]. In our study, all three misdiagnosed tumors (cases 10–12) were evaluated by using only IHC. Moreover, given that tumors may be dMMR or MSI but not the other, dual testing could indeed be considered to minimize incorrect treatment decisions. If discordance is observed, cases should be promptly and comprehensively evaluated. However, it remains to be established if this approach is cost- and time-effective.

In LS-unrelated cancers, the ESMO guideline recommends NGS [42]. Our data support the relevance of NGS in this group, as we found that discordance between dMMR status and MSI was mainly seen in these cancers. Notably, NGS is becoming increasingly available to clinical laboratories as a scalable and cost-effective method to evaluate genomic alterations in parallel, making it a potential new routinely used test in TMB and MSI detection for all tumor types and thereby paving the way for precision oncology.

The strength of this study lies in its tumor-agnostic setting. Moreover, in contrast to previous studies evaluating concordance between different methodologies [6,9–16], we extensively reviewed discordant cases. After this, only a few true discordant cases remained. However, the study also has limitations inherent to its retrospective nature. First, material from routine care could not always be retrieved. Second, routine diagnostics and WGS were not necessarily performed on the same tissue. We therefore could not always exclude the existence of tumor heterogeneity. However, in the majority of cases, we had reliable alternative explanations for the discordance. Lastly, as our dataset was limited to patients with dMMR/MSI tumors as determined by routine diagnostics, we could not evaluate the overall accuracy of current diagnostics and the number of dMMR/MSI tumors currently misdiagnosed as pMMR/MSS. This may occur, for example, due to retained MMR protein expression due to MMR missense variants disrupting function but not expression [43,44].

In conclusion, in these patients initially diagnosed with dMMR/MSI tumors by routine diagnostics, the true assay-based discordance rate between routine dMMR/MSI diagnostics and WGS was relatively low (5%) and caused by dMMR tumors that did not harbor an MSI molecular phenotype. When assessing patient eligibility for ICB, clinicians and pathologists should be aware of the risk of MPTs and the limitations of different tests.

Acknowledgements

The DRUP team would like to thank the Stelvio for Life Foundation and the Dutch Cancer Society for their financial support; AstraZeneca and Bristol Myers Squibb for

providing durvalumab and nivolumab, respectively, and financial support; the Center for Personalized Cancer Treatment; the Multidisciplinary Expert Board for supporting the central case-review process; the Independent Data Monitoring Committee for their advice on cohort decisions and the monitoring of preliminary safety data; Hartwig Medical Foundation for their in-kind support by providing sequencing on pretreatment biopsies; Palga (Dutch Pathology Registry) for providing data and collection of specimens; The Netherlands Cancer Institute's Core Facility Molecular Pathology & Biobanking (CFMBP) for supplying NKI-AVL Biobank material and lab support, and the Scientific Department and Pharmacy for their facilitating services; J Westra and JJM Schoep for their facilitating services; MM Lange and E van den Broek for their contributions to the assessment of immunohistochemical stains; MJA de Jonge, LA Devriese, GA Cirkel, DJA de Groot, A Hoeben, LV Beerepoot, ED Kerver, HM Westgeest, AD Bins, G Vreugdenhil, T van Voorthuizen, AJE Vulink, FLG Erdkamp, JM van Rooijen, D Houtsma, H de Graaf, P de Mol, MP Hendriks, JWB de Groot, M Los, S Boudewijns, EJM Siemerink, and FJF Jeurissen for their contributions to trial recruitment; and lastly, all the patients, investigators and research staff from all participating hospitals. DRUP is supported by the Stelvio for Life Foundation (grant number not applicable); the Dutch Cancer Society (grant number 10014); and all participating pharmaceutical companies (grant numbers not applicable): Amgen, AstraZeneca, Bristol Myers Squibb, Eisai, GlaxoSmithKline, Janssen, Eli Lilly, Novartis, Pfizer, and Roche.

Author contributions statement

BSG, HMWV, HG, PS and EEV were responsible for the conceptualization and study design. BSG, LJZ, JMBH, LRH, HW, GFW, ACS, PR, AMLJ, WWJL, AB, ML and CMLH were responsible for the provision of study materials or patients. BSG, LJZ, JMBH, HW, LRH, GFW and ACS were responsible for collection and assembly of data. BSG, DMB, TWB and PS were responsible for data analysis and interpretation. All authors have read, revised and approved the article.

Data availability statement

All the data described in this study are freely available for academic use upon request from the corresponding author. WGS data can be obtained from the Netherlands Cancer Institute and Hartwig Medical Foundation through standardized procedures and request forms. These can be found at https://www.hartwigmedicalfoundation.nl/en. For further information, see van der Velden [45].

References

1. Bonneville R, Krook MA, Kautto EA, *et al*. Landscape of microsatellite instability across 39 cancer types. *JCO Precis Oncol* 2017; **2017:** PO.17.00073.
2. McConechy MK, Talhouk A, Li-Chang HH, *et al*. Detection of DNA mismatch repair (MMR) deficiencies by immunohistochemistry can effectively diagnose the microsatellite instability (MSI) phenotype in endometrial carcinomas. *Gynecol Oncol* 2015; **137:** 306–310.
3. Marabelle A, Le DT, Ascierto PA, *et al*. Efficacy of pembrolizumab in patients with noncolorectal high microsatellite instability/mismatch repair-deficient cancer: results from the phase II KEYNOTE-158 study. *J Clin Oncol* 2020; **38:** 1–10.
4. Germano G, Lamba S, Rospo G, *et al*. Inactivation of DNA repair triggers neoantigen generation and impairs tumour growth. *Nature* 2017; **552:** 116–120.
5. Evrard C, Tachon G, Randrian V, *et al*. Microsatellite instability: diagnosis, heterogeneity, discordance, and clinical impact in colorectal cancer. *Cancers (Basel)* 2019; **11:** 1567.
6. Guyot D'Asnieres De Salins A, Tachon G, Cohen R, *et al*. Discordance between immunochemistry of mismatch repair proteins and molecular testing of microsatellite instability in colorectal cancer. *ESMO Open* 2021; **6:** 100120.
7. Lin JH, Chen S, Pallavajjala A, *et al*. Validation of long mononucleotide repeat markers for detection of microsatellite instability. *J Mol Diagn* 2022; **24:** 144–157.
8. Suraweera N, Duval A, Reperant M, *et al*. Evaluation of tumor microsatellite instability using five quasimonomorphic mononucleotide repeats and pentaplex PCR. *Gastroenterology* 2002; **123:** 1804–1811.
9. Shimozaki K, Hayashi H, Tanishima S, *et al*. Concordance analysis of microsatellite instability status between polymerase chain reaction based testing and next generation sequencing for solid tumors. *Sci Rep* 2021; **11:** 20003.
10. Bai H, Wang R, Cheng W, *et al*. Evaluation of concordance between deficient mismatch repair and microsatellite instability testing and their association with clinicopathological features in colorectal cancer. *Cancer Manag Res* 2020; **12:** 2863–2873.
11. Loughrey MB, McGrath J, Coleman HG, *et al*. Identifying mismatch repair-deficient colon cancer: near-perfect concordance between immunohistochemistry and microsatellite instability testing in a large, population-based series. *Histopathology* 2021; **78:** 401–413.
12. Zhang L. Immunohistochemistry versus microsatellite instability testing for screening colorectal cancer patients at risk for hereditary nonpolyposis colorectal cancer syndrome. Part II. The utility of microsatellite instability testing. *J Mol Diagn* 2008; **10:** 301–307.
13. Saeed OAM, Mann SA, Luchini C, *et al*. Evaluating mismatch repair deficiency for solid tumor immunotherapy eligibility: immunohistochemistry versus microsatellite molecular testing. *Hum Pathol* 2021; **115:** 10–18.
14. Stelloo E, Jansen AML, Osse EM, *et al*. Practical guidance for mismatch repair-deficiency testing in endometrial cancer. *Ann Oncol* 2017; **28:** 96–102.
15. Malapelle U, Parente P, Pepe F, *et al*. Evaluation of micro satellite instability and mismatch repair status in different solid tumors: a multicenter analysis in a real world setting. *Cells* 2021; **10:** 1878.
16. Matsubayashi H, Oishi T, Sasaki K, *et al*. Discordance of microsatellite instability and mismatch repair immunochemistry occurs depending on the cancer type. *Hum Pathol* 2023; **135:** 54–64.
17. Jaffrelot M, Fares N, Brunac AC, *et al*. An unusual phenotype occurs in 15% of mismatch repair-deficient tumors and is associated with non-colorectal cancers and genetic syndromes. *Mod Pathol* 2022; **35:** 427–437.
18. Leclerc J, Vermaut C, Buisine MP. Diagnosis of Lynch syndrome and strategies to distinguish Lynch-related tumors from sporadic MSI/dMMR tumors. *Cancers (Basel)* 2021; **13:** 467.

19. Le DT, Uram JN, Wang H, *et al*. PD-1 blockade in tumors with mismatch-repair deficiency. *N Engl J Med* 2015; **372:** 2509–2520.
20. Overman MJ, McDermott R, Leach JL, *et al*. Nivolumab in patients with metastatic DNA mismatch repair-deficient or microsatellite instability-high colorectal cancer (CheckMate 142): an open-label, multicentre, phase 2 study. *Lancet Oncol* 2017; **18:** 1182–1191.
21. Trullas A, Delgado J, Genazzani A, *et al*. The EMA assessment of pembrolizumab as monotherapy for the first-line treatment of adult patients with metastatic microsatellite instability-high or mismatch repair deficient colorectal cancer. *ESMO Open* 2021; **6:** 100145.
22. Marcus L, Lemery SJ, Keegan P, *et al*. FDA approval summary: pembrolizumab for the treatment of microsatellite instability-high solid tumors. *Clin Cancer Res* 2019; **25:** 3753–3758.
23. Cohen R, Duval A, Svrcek M. Primary resistance to immune checkpoint inhibitors in metastatic colorectal cancer – beyond the misdiagnosis – in reply. *JAMA Oncol* 2019; **5:** 741.
24. Eisenhauer EA, Therasse P, Bogaerts J, *et al*. New response evaluation criteria in solid tumours: revised RECIST guideline (version 1.1). *Eur J Cancer* 2009; **45:** 228–247.
25. Casparie M, Tiebosch AT, Burger G, *et al*. Pathology databanking and biobanking in The Netherlands, a central role for PALGA, the nationwide histopathology and cytopathology data network and archive. *Cell Oncol* 2007; **29:** 19–24.
26. Priestley P, Baber J, Lolkema MP, *et al*. Pan-cancer whole-genome analyses of metastatic solid tumours. *Nature* 2019; **575:** 210–216.
27. Roepman P, de Bruijn E, van Lieshout S, *et al*. Clinical validation of whole genome sequencing for cancer diagnostics. *J Mol Diagn* 2021; **23:** 816–833.
28. Blokzijl F, Janssen R, van Boxtel R, *et al*. MutationalPatterns: comprehensive genome-wide analysis of mutational processes. *Genome Med* 2018; **10:** 33.
29. Forbes SA, Beare D, Boutselakis H, *et al*. COSMIC: somatic cancer genetics at high-resolution. *Nucleic Acids Res* 2017; **45:** D777–D783.
30. Schipper LJ, Samsom KG, Snaebjornsson P, *et al*. Complete genomic characterization in patients with cancer of unknown primary origin in routine diagnostics. *ESMO Open* 2022; **7:** 100611.
31. Cantwell-Dorris ER, O'Leary JJ, Sheils OM. $BRAF^{V600E}$: implications for carcinogenesis and molecular therapy. *Mol Cancer Ther* 2011; **10:** 385–394.
32. Andrici J, Goeppert B, Sioson L, *et al*. Loss of BAP1 expression occurs frequently in intrahepatic cholangiocarcinoma. *Medicine (Baltimore)* 2016; **95:** e2491.
33. Shia J. The diversity of tumours with microsatellite instability: molecular mechanisms and impact upon microsatellite instability testing and mismatch repair protein immunohistochemistry. *Histopathology* 2021; **78:** 485–497.
34. Helderman NC, Bajwa-Ten Broeke SW, Morreau H, *et al*. The diverse molecular profiles of Lynch syndrome-associated colorectal cancers are (highly) dependent on underlying germline mismatch repair mutations. *Crit Rev Oncol Hematol* 2021; **163:** 103338.
35. Helderman NC, Van Der Werf-'t Lam AS, MSH6 TUMOR GROUP, *et al*. Molecular profile of MSH6-associated colorectal carcinomas shows distinct features from other Lynch syndrome-associated colorectal carcinomas. *Gastroenterology* 2023; **165:** 271–274.e2.
36. Mandal R, Samstein RM, Lee KW, *et al*. Genetic diversity of tumors with mismatch repair deficiency influences anti-PD-1 immunotherapy response. *Science* 2019; **364:** 485–491.
37. Fujimoto A, Fujita M, Hasegawa T, *et al*. Comprehensive analysis of indels in whole-genome microsatellite regions and microsatellite instability across 21 cancer types. *Genome Res* 2020; **30:** 334–346.
38. Bacher JW, Udho EB, Strauss EE, *et al*. A highly sensitive pan-cancer test for microsatellite instability. *J Mol Diagn* 2023; **25:** 806–826.
39. Yu F, Makrigiorgos A, Leong KW, *et al*. Sensitive detection of microsatellite instability in tissues and liquid biopsies: recent developments and updates. *Comput Struct Biotechnol J* 2021; **19:** 4931–4940.
40. Anandappa G, Overman MJ. Harnessing the therapeutic vulnerability of MMR heterogeneity in colorectal cancer. *Cell Rep Med* 2023; **4:** 100908.
41. Vogt A, Schmid S, Heinimann K, *et al*. Multiple primary tumours: challenges and approaches, a review. *ESMO Open* 2017; **2:** e000172.
42. Luchini C, Bibeau F, Ligtenberg MJL, *et al*. ESMO recommendations on microsatellite instability testing for immunotherapy in cancer, and its relationship with PD-1/PD-L1 expression and tumour mutational burden: a systematic review-based approach. *Ann Oncol* 2019; **30:** 1232–1243.
43. Hechtman JF, Rana S, Middha S, *et al*. Retained mismatch repair protein expression occurs in approximately 6% of microsatellite instability-high cancers and is associated with missense mutations in mismatch repair genes. *Mod Pathol* 2020; **33:** 871–879.
44. Chen W, Hampel H, Pearlman R, *et al*. Unexpected expression of mismatch repair protein is more commonly seen with pathogenic missense than with other mutations in Lynch syndrome. *Hum Pathol* 2020; **103:** 34–41.
45. van der Velden DL, Hoes LR, van der Wijngaart H, *et al*. The drug rediscovery protocol facilitates the expanded use of existing anticancer drugs. *Nature* 2019; **574:** 127–131.

SUPPLEMENTARY MATERIAL ONLINE

Table S1. Average relative contribution of single-base substitution signatures associated with dMMR/MSI in WGS-based MSI tumors ($n = 108$)

Table S2. Relative contribution of signatures associated with dMMR/MSI in WGS-based MSS tumors